Transition from diffusing to dynamic light scattering in solutions of monodisperse polystyrene spheres

Matthew F. Clapper, Joseph S. Collura, Daniel Harrison,* and Michael R. Fisch
Department of Physics, John Carroll University, University Heights, Ohio 44118
(Received 12 March 1998; revised manuscript received 8 October 1998)

Light scattering in the backscattering geometry, and transmission measurements are used to size monodisperse spherical particles in solutions. The concentration of spheres spans the scattering to range from single scattering to very highly multiple scattering. These experiments were performed by varying volume fractions of polystyrene latex spheres of nominal diameter 0.136 and 1.015 μm. Transmission measurements were performed as a function of particle size, volume fraction, and sample thickness with a spectrophotometer equipped with an integrating sphere. The data show that for thin samples the percent transmission is nearly independent of particle size and depends only on L/l^*, the ratio of the sample thickness L to the transport mean free path l^*. By fitting the autocorrelation functions of samples obtained from known sphere sizes to a generalized cumulants model, which describes both the highly multiple scattering regime and the singly scattering regime, parameters were found that allow particle sizes to be determined over a wide range of scattering strengths. For samples of unknown size, this method can size monodisperse spherical particles in highly scattering solutions to better than 10%.
[S1063-651X(99)14302-2]

PACS number(s): 42.25.Bs, 42.25.Fx, 78.35.+c, 78.20.Ci

I. INTRODUCTION

Within the past 10–15 years, diffusing wave spectroscopy DWS, a technique for measuring the size of particles in samples that are highly scattering has been developed [1–10]. DWS works in the regime where photons are scattered many, many times before being detected. The analysis of intensity-intensity autocorelation functions, $G_2(t) \equiv \langle I(t')I(t'+t)\rangle$ in this case is based on two fundamental approximations. The first approximation assumes that due to the very large number of scattering events, the photon path may be described as a random walk. It neglects interference effects of the light, assuming that the scattering is not so strong as to approach the localization of light due to random scattering, and assumes that the light diffuses through the sample [11]. The diffusion approximation makes it possible to calculate the distribution of paths taken by photons through the medium, allowing the dynamics of the medium to be treated by statistical calculations. The second approximation assumes that individual scattering events can be replaced by an average scattering event. Then using the diffusion approximation the total path length and the number of average scattering events are found. There are two common experimental geometries used for such experiments, transmission and backscattering. Of these two, backscattering is better suited to particle sizing because the transport mean free path l^* need not be determined independently to analyze the autocorrelation function.

The goal of the experiments described in this article was to develop a method of sizing nearly monodisperse spherical particles over a wide range of scattering strengths, from the strongly multiply scattering to the approximately singly scattering regime. This goal was achieved by a combination of quasielastic light scattering spectroscopy in the backscattering geometry and transmission measurements which were used to determine the transport mean free path l^*. The modeled time dependence of the measured autocorrelation functions contained several parameters that are functions of l^*/L, where L is the sample length, or as will be demonstrated, a function of the fraction of light transmitted through the sample, but not the mean size of the spheres. These experiments extend in a different direction the diffuse-transmission spectroscopy experiments of Kaplan *et al.* [12].

II. THEORY

A. Multiple light scattering

Multiple light scattering has been and continues to be of great theoretical and practical interest. The literature in this field is spread over a wide range of disciplines including astrophysics, biomedical imaging, and atmospheric science to name a few. Thus, it is difficult to be comprehensive in one's reference to the literature. An introductory review is provided by Bohren [13]. The monographs by Chandrasekhar [14], van de Hulst [15], and Ishimaru [16] all discuss the theory in great detail. van de Hulst's two volume monograph is particularly useful in the present context because it contains a great many tables. This problem continues to be of great interest as recent work by Kolinko *et al.* [17], Bailey and Cannell [18], and Stark and Lubensky [19] indicate. However, all of these monographs and articles indicate that multiple light scattering calculations are difficult, computationally intensive, and time consuming. For this reason our experimental results on the total light scattered will be compared to the tables in van de Hulst [20].

The following approximate approach is used in the present work. Since the particles are essentially monodisperse polystyrene spheres, a very dilute solution of the par-

*Also at Department of Physics, Case Western Reserve University, Cleveland, OH 44106.

ticles was sized using both quasielastic and static light scattering techniques. The quasielastic light scattering data were taken at a scattering angle of 90° and the static light scattering data was taken at 1° intervals between 20 and 138°. The quasielastic light scattering data was fit to a third-order cumulants fit [21] and the static light scattering data fit to Mie's theory [22]. In this later calculation the indices of refraction of water and polystyrene were taken from Kerker [23]. The sizes measured by dynamic and static light scattering were consistent with those on the bottle and were also consistent with the stated polydispersity.

On the basis of these results and upon the assumption of nonabsorbing spheres [22] the extinction cross section C_{ext}, scattering cross section C_{sca}, and efficiency of radiation pressure cross section C_{pr}, were calculated (in the present case we assume no absorption so that $C_{\text{ext}}=C_{\text{sca}}$);

$$C_{\text{pr}}=C_{\text{ext}}-C_{\text{sca}}\langle\cos(\theta)\rangle, \tag{1}$$

where $\langle\cos(\theta)\rangle$ [22] is the asymmetry parameter which is a measure of how much of the scattered light is scattered nonisotropically. That is, $\langle\cos(\theta)\rangle$ is zero for isotropic scattering, greater than zero for excess scattering in the forward direction and less than zero for scattering predominantly directed backwards.

Systems which scatter light strongly are characterized by two lengths that are obtained from these cross sections. The scattering mean free path l, which measures the average distance a photon travels before scattering, and the transport mean free path l^*, which measures the distance beyond which the direction of propagation of the photon is randomized. These are related to the above cross sections as follows:

$$l=\frac{1}{nC_{\text{sca}}(1-H)}, \tag{2}$$

$$l^*=\frac{l}{(1-\langle\cos(\theta)\rangle)(1-H)}, \tag{3}$$

where n is the number of spheres per unit volume and H is the volume fraction of spheres [16].

The scattering cross section of the spheres used in the present study are rather complex functions of the scattering angle. Following van de Hulst [20], the actual scattering cross section was replaced by a simpler one. This is based on the fact that the two characteristics of the single scattering are its albedo (defined as the ratio of the scattering cross section to the total or extinction cross section) and the asymmetry parameter, $g\equiv\langle\cos(\theta)\rangle$. A simple phase function that is often used is the Henyey-Greenstein (HG) function [15,16]. The phase function is related to the scattering cross section through $C_{\text{sca}}=C_{\text{ext}}$ (phase function). The asymmetry parameter of the HG phase function is g, and the extinction cross section can be calculated from the Mie theory, thus this function can be used to at least roughly approximate the more complex Mie result. The next approximation was first noted by van de Hulst. This approximation states that for nonabsorbing particles the fraction of an infinite plane wave that is transmitted through a sample of optical thickness, is approximately a universal function of l^*. In fact, this is verified by both his numerical calculations [20] and the experiments discussed later in this paper. This observation allows one to determine l^* from the transmitted intensity in the weakly scattering regime, the intermediate regime and the multiple scattering regime. As will be shown later the transport mean free path length is an important parameter in the description of the quasielastically scattered light, and will be used as an independent variable in the formal description of our results.

B. Quasielastic light scattering

Since detailed derivations of all of the theoretical forms which will be discussed are in the literature [25–29], this section will simply summarize the important results. The autocorrelation function of light scattered from a dilute weakly scattering solution of particles, which has a fairly narrow distribution of sizes, may be analyzed using the method of cumulants. This technique is widely discussed, and was first described by Koppel [21]. In this model the normalized autocorrelation function is described by the following function:

$$g_2(t)=\frac{(G_2(t)-\langle I\rangle^2)}{\langle I\rangle^2}\approx A\exp(-K_1t+1/2K_2t^2+\cdots), \tag{4}$$

where $g_2(t)$ is the experimentally determined normalized correlation function, A is its amplitude (which is very close to 1.00), $K_1=2\langle D\rangle q^2$, where $\langle D\rangle$ is the mean diffusion coefficient of the particles, q is the scattering vector, $q=4\pi n/\lambda\sin(\theta/2)$, where n is the index of refraction of the solution, λ the vacuum wavelength of the incident light, and K_2 is related to the width of the particle distribution function. Using the obtained (through fitting) value of K_1 and the Stokes-Einstein relation [26], the particle size can then be found.

In highly multiple scattering theory, different approximations are made but again the final goal in particle sizing is to fit the autocorrelation function and relate the coefficients unambiguously to the particle size. Here a number of approximations are necessary. Pine and Weitz [10] describe a relatively simple model that fits data obtained in the backscattering geometry. The actual situation may be more complex than their simple form would indicate. See, for example, MacKintosh and John [30], Durian [31,32], Stephen and Cwilich [33], Stephen [34], Maret and Wolf [35], and Edrei and Kaveh [36].

In the multiple scattering region, experimentally determined normalized correlation functions are well fitted to a cumulants expansion of the form used by Fraden and Maret [3]:

$$g_2(t)=A\exp\left(-2\gamma\sqrt{\frac{6t}{\tau}}+ct\right), \tag{5}$$

where A is a constant, γ is a fitting parameter which will be discussed in greater detail below, τ is the single back scattering time, $\tau=(1/\langle D\rangle)(2\pi n/\lambda)^2$, and c is a constant. In the present study we need a theoretical model that will allow a broad range of autocorrelation functions from those describing dilute weakly scattering samples to multiple scattering without any *a priori* knowledge of the sample. In order to analyze correlation functions obtained over a broad range of concentrations without changing the theoretical form, we

combined the dilute cumulant form, Eq. (4), and the multiple scattering cumulant form, Eq. (5), to produce the following empirical model for $g_2(t)$:

$$g_2(t)=A\exp(-f\sqrt{t}+ct-dt^2), \tag{6}$$

where A, c, d, and f are all constants. When applying this form to highly multiple scattering samples one would anticipate $|c/f^2|<1$, and d to be negligible, while for very weakly scattering samples $|c/f^2|\gg 1$ and $|d/f^2|<1$. These expectations are experimentally verified.

When correlation functions from highly multiple scattering samples are analyzed using Eq. (6) the fitting parameter f can be combined with the theoretically predicted τ to determine the coefficient γ. By simultaneously looking at Eq (5) and Eq. (6) and comparing like coefficients of t^n we obtain

$$f=2\gamma\sqrt{\frac{6}{\tau}}. \tag{7}$$

Later we will experimentally show that γ is independent of particle size and apparently a function of only l^*, as predicted. Thus, knowing γ Eq. (7) may be solved for τ and the particle size determined.

In the weakly scattering limit, comparison of Eq. (4) and Eq. (6) allows one to show that $c=2Dq^2$. Thus, once more particle size may be determined as when using Eq. (6). In principle and in practice, the ratio of the two coefficients c and d may be used to determine the ''polydispersity parameter.'' In general, a fourth term K_3t^3 must be added to Eq. (4) when this is done. For this reason the polydispersity was not explicitly calculated even for weakly scattering samples.

An alternate approach to the evaluation of autocorrelation functions obtained from a wide range of scattering strengths is given by Koňák *et al.* [37] and Štěpánek [38]. Štěpánek's quasielastic light scattering experiment was conducted at a number of scattering angles rather than at one fixed angle near 180° as in the present experiment. His analysis indicates that at very small volume fractions of polystyrene spheres, there is one unimodal range of decay times. In an intermediate range of volume fractions (and hence scattering strengths) a bimodal distribution occurs with the second component occurring at faster times than the component observed in more dilute solutions. At high concentrations only this faster mode is observed. In the present context a similar model can be formed in which the two cumulant forms [Eqs. (4) and (5)] are added:

$$g_2(t)=(A_fe^{(-f\sqrt{t}-ct)}+A_se^{(-dt+gt^2)})^2+b, \tag{8}$$

where A_f is the amplitude of the fast mode, A_s the amplitude of the slow mode, b is the optional background fitting parameter, and f, c, d, and g are fitting parameters that will be related to the particle size as discussed above.

III. EXPERIMENTAL APPARATUS AND PROCEDURE

Two experimental apparatus were used in this research. The first was a commercial Perkin-Elmer Lambda–40P spectrophotometer with a Labsphere RSA-PE-20 integrating sphere that was used to measure the total transmission (diffusely scattered plus direct) as a function of wavelength. The transmission was measured for samples of mass fraction M, $5\times10^{-5}\leqslant M\leqslant 0.1$ for the 0.126-mm spheres and $2.5\times10^{-5}\leqslant M\leqslant 0.1$ for the 0.966-μm spheres. The mass fraction was converted to number of particles per unit volume n. The transport mean free path l^* was calculated using Eq. (3). This allowed the transmission to be evaluated as a function of the dimensionless parameter L/l^*.

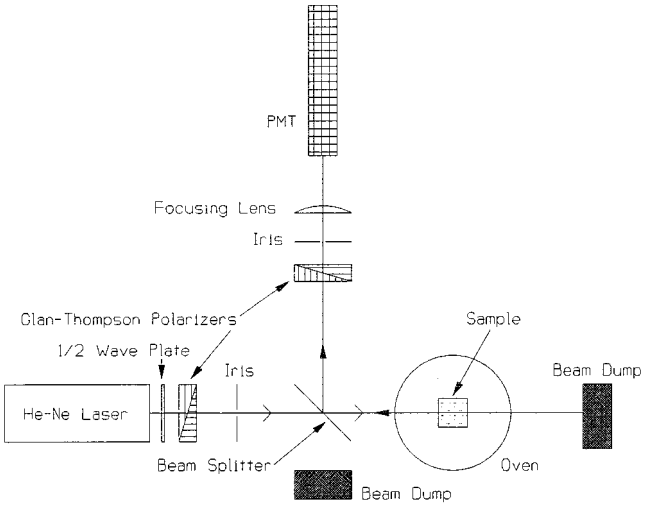

FIG. 1. Diagram of the experimental apparatus.

A typical procedure for transmission measurements consisted of measuring the transmission for several path lengths. One of the approximations of the theory is that the scattering layer must be very wide compared to the optical thickness. Thus, strongly scattering samples in thick (1-cm) sample holders would not work well, while in weakly scattering samples such sample holders were preferred.

The relevant components of the backscattering apparatus, shown schematically in Fig. 1, are the laser and polarization optics, a pellicle beamsplitter, sample oven, collection optics and photomultiplier tube, and 64-channel correlator interfaced to a computer. This is the standard 45° beam-splitter geometry often used for coherent back scattering measurements [39]. The laser is a Spectra-Physics 60-mW Helium-Neon laser, with output wavelength of 632.8 nm. This power is sufficient for the present experiments and did not inadvertently heat the sample. Due to space constraints a mirror is used to redirect the beam 90° from its initial direction and along the subsequent optical beam line. Immediately following the mirror along the beampath is a $\frac{1}{2}$ wave plate in a rotation stage followed by a Glan-Thompson polarizer oriented to pass vertically polarized light. The $\frac{1}{2}$ wave plate-polarizer combination provides a continuous attenuator of the intensity while preserving vertical polarization of the light incident on the sample [40]. This variable attenuator is followed by an iris that helps to remove stray light near the circumference of the beam.

Following the iris, a 1-in. pellicle beamsplitter is kinematically mounted and positioned at a 45° angle to the incident beam so it can transmit the beam to the sample stage as well as reflect backscattered radiation from the sample to the collection optics and photomultiplier tube (PMT). The sample oven is a brass cylinder with a square hole, designed to hold a standard 1 cm (inside thickness) square cuvette,

aligned parallel to the oven's long axis. In order to allow the beam to irradiate the sample and scattered light to be collected, a semicylindrical wedge was machined out of the oven. Finally, a small hole is drilled through the back of the oven to allow transmitted light to pass through the sample stage. The cuvette is rotated so that the reflected beam is translated off the incident beampath since only the backscattered signal is needed.

There are two beamstops in the apparatus. These are used to minimize any unwanted light being reflected off surfaces and back into the beampath. Finally, the collection optics consist of a focusing lens, a PMT and another Glan-Thompson polarizer oriented parallel to the previous polarizer. The PMT is a Malvern Instruments photomultiplier tube and preamplifier removed from a Zetasizer I and modified to hold a focusing lens and iris. Further details are available elsewhere [41].

The samples, obtained from Duke Scientific Corporation, were polystyrene latex spheres of nominal mean diameter 0.126 and 0.966 μm. The samples were prepared in the following manner. First, the sample stock was placed into an ultrasonic cleaner to help break up any aggregated particles and then gently stirred to prevent foaming as was recommended by Duke Scientific. No other filtration process was used on the stock sample. The water used to dilute the original sample was obtained from a Millipore Milli-RO water purification system which produced water of resistivity up to 0.2 MΩ cm. The water was filtered with a 0.2-μm inorganic membrane filter before combining it with the polystyrene sample. All quartz cuvettes were flushed with clean water many times to remove excess material after each run. The cuvettes were then flushed with toluene to dissolve any trapped polystyrene, rinsed with acetone and then finally ethanol before air drying. All experiments were conducted at room temperature, and the temperature was recorded for each sample run. The autocorrelation functions were analyzed using the method of Harrison and Fisch [42].

IV. EXPERIMENTAL RESULTS

Quasielastic and static light scattering measurements were used to measure the size of the polystyrene sphere-water samples. The mean diameter of the two different size spheres used were 136 and 1015 nm. The smaller size is large enough to give multiple scattering at the concentration supplied by the manufacturer, yet still had an asymmetry parameter g very close to zero. Actual calculation yield the value $g=0.03$ for the 136-nm-diam spheres. The value of g for the 1015-nm spheres is approximately 0.88, which is very close to the maximum value obtainable in nonabsorbing spheres [24]. These measured size values were used in all calculations that included the particle size. The percent transmission was measured in the Lambda-40P spectrometer at wavelengths between 400 and 900 nm. From this data the value of the percent transmission at 633 nm was obtained. This wavelength was chosen because it is the wavelength of the laser used in the quasielastic light scattering studies. From the calculated scattering cross section of monodisperse spheres of the appropriate diameter and for a wavelength of 633 nm and the known values of n, the number of spheres per unit volume, and the asymmetry factor, g, the transport mean free path was calculated using Eq. (3). The resulting graph of percent transmission versus the dimensionless parameter L/l^* is shown in Fig. 2.

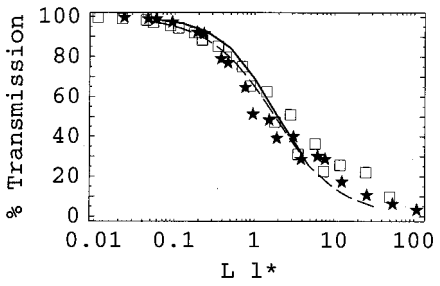

FIG. 2. Percent transmission as a function of L/l^*. The solid curve is the prediction for $g=0.875$ and the dashed curve the prediction for $g=0$. Squares and stars are experimental data: □, 0.136-μm-diam spheres; ★, 1.015-μm-diam spheres.

To obtain the percent transmitted shown in this figure the following procedure was followed. First, the percent of light transmitted was measured for several values of L but different l^* such that L/l^* was constant. Semilogarithmic graphs of percent light transmitted versus L at a wavelength of 633 nm were constructed. These graphs were typically very linear. On the basis of this linear behavior the percentage of light transmitted was extrapolated to $L\rightarrow 0$. The percent transmitted at $L\rightarrow 0$ was used because the theory assumes that the beam irradiating the sample is infinite compared to the thickness of the sample. Clearly this procedure was important for very strongly scattering samples; however, experimentally the effect was very small for weakly scattering samples. The two dashed curves on this graph are the Henyey-Greenstein model prediction based on radiation transfer theory [24], for both spheres. Notice that there is not perfect agreement between the two model curves. However, the experimental data is in good agreement with the model predictions. This graph shows that the dependence of the percent transmission on L/l^* is independent of both the asymmetry parameter of the particle and, more significantly, the particle size. The significance of this result is that it allows the value of l^* of suspensions of monodisperse spheres in the range studied to be experimentally determined simply by measuring the total transmission of light through the sample of thickness known L.

The quasielastic light scattering data was analyzed using the single cumulant model, Eq. (6) and the sum of cumulant model, Eq. (8). The resulting chi-squares of both of the fits were analyzed at each concentration using the F test [43]. The results of this test indicate that both models fit to the data are equally acceptable in the difficult to analyze middle region where both single and some multiple scattering exist. The sum of cumulants model, Eq. (8) yields somewhat better χ^2 at both the highly multiple scattering and the very weakly scattering limits. However, the fits to the single cumulants model form an overall better picture. That is to say, the behavior of γ and the ratio of the predicted single decay time to the fitted decay time vary much more systematically with l^* in this type of fit.

The fitted parameters from the single cumulant fit to the intensity autocorrelation functions, and the particle size independently determined in very dilute solutions were used to

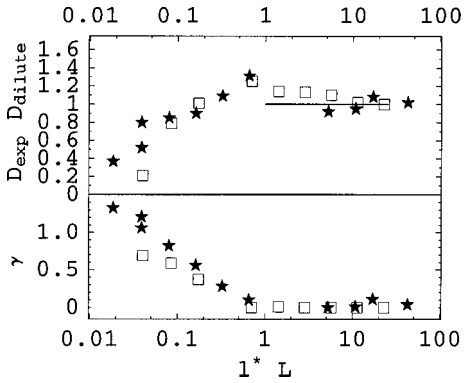

FIG. 3. $D_{\mathrm{exp}}/D_{\mathrm{dilute}}$ and γ as a function of l^*/L for the modified cumulant fit. The solid line in the top panel corresponds to $D_{\mathrm{exp}}=D_{\mathrm{dilute}}$. The symbols have the same meaning as in Fig. 2.

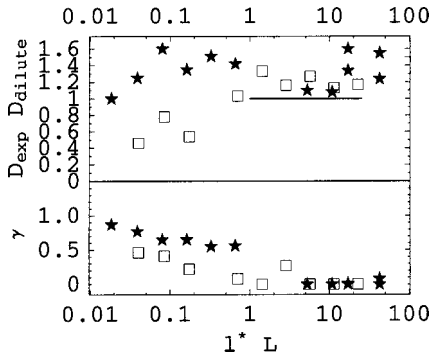

FIG. 4. $D_{\mathrm{exp}}/D_{\mathrm{dilute}}$ and γ as a function of l^*/L for the sum of cumulant fits. The solid line and symbols have the same meaning as in Fig. 3.

calculate γ, and the ratio of the diffusion coefficient, $D_{\mathrm{exp}}/D_{\mathrm{dilute}}$. In this last expression D_{exp} is the diffusion coefficient determined from the coefficient of the linear term in time in the cumulant fit and D_{dilute} is the diffusion coefficient determined in very dilute solutions at a scattering angle of 90°, and calculated using the measured size and the Stokes-Einstein equation. These two parameters, obtained from fitting backscattering geometry correlation functions appeared to be systematic functions of the function of transport mean free path, l^*/L. Figure 3 is a graph of γ and $D_{\mathrm{exp}}/D_{\mathrm{dilute}}$ as a function of l^*/L calculated using Eq. (3). In the highly multiple scattering regime γ ranges between 1.26 and 0.75, and decreases with increasing l^*/L throughout this region. The values of the ratio of diffusion coefficients approaches one at approximately the same value of l^*/L at which γ falls below approximately 0.4.

It is important to observe that this theoretical form provides a smooth transition between the highly multiple scattering and the single scattering regimes for both sizes of spheres, allowing almost any solution of monodisperse spheres within this region to be sized. For very large values of l^*/L the parameters of the fit indicate that in the model the coefficient f is very small and the data is very well represented by Eq. (4), as expected. For small values of l^*/L the parameters are such that the linear term is a small correction to the $\sqrt{t}$ term and the data could just as easily be fit using Eq. (5) with $c\equiv 0$.

The analysis based on the sum of two exponentials, Eq. (8) also fits rather well. However, not surprisingly the fitting parameters are somewhat different than in the fits to a single cumulants functional form. Once more the γ needed to fit the data is a function of l^*/L. In this case the value of γ obtained for the two different sizes are very different. It is not clear that there is a single systematic relationship between γ and l^*/L except at large l^*/L where γ approaches zero. The situation with the diffusion coefficient is equally problematic. For instance, even in very dilute solutions where $D_{\mathrm{exp}}/D_{\mathrm{dilute}}$ should approach one, the data is systematically high by 20% or more and rather noisy. Thus, this does not appear to be a good model for determining particle sizes. These results are shown in Fig. 4.

In order to test the conclusion that there was a single empirical relationship between both γ and $D_{\mathrm{exp}}/D_{\mathrm{dilute}}$ and l^*/L two samples were prepared. Both were of mass fraction $M=0.1$. The nominal diameters of the spheres were 0.330 and 0.724 μm, respectively. The concentration was chosen to be clearly not highly multiple scattering and yet not so dilute to be single scattering either. The percent transmission for each sample was approximately 70% through a 1-mm cuvette. Using the data summarized in Fig. 3, γ is expected to be very close to zero and the coefficient of the linear term in time in the fit should equal Dq^2, where D is the diffusion coefficient of the particles the particles and q is the backscattering wave vector. Using these ideas the diffusion coefficient for the 0.325-μm sample was calculated to be 1.26×10^{-8} cm^2/s. Using the Stokes-Einstein equation, the corresponding size was calculated to be 0.40 μm. The diffusion coefficient for the 0.724-mm sample was calculated to be 6.95×10^{-9} cm^2/s. The size of the particles was calculated to be 0.725 μm. The error in the smaller particles was much greater than that of the larger particles, however, the 0.325-μm stock sample had a previous tendency to aggregate, which is consistent with this larger experimentally determined size.

V. CONCLUSION

An accurate method to size spherical, monodisperse, particles ranging from the single scattering regime through the very highly multiple scattering regime has been developed and tested. This method does not require any special instrumentation other than standard light scattering apparatus in the backscattering geometry. Two models, an empirical modified cumulants form given by Eq. (6), and a model suggested by Štěpánek, which is essentially a sum of cumulants given by Eq. (8), have been evaluated and found to adequately represent the data. The modified cumulants model has been shown from our analysis to obtain more physically reasonable results although, from a data fitting perspective, the sum of cumulants is equally good. Applications of this technique will allow evaluation of particle sizing in light scattering experiments at almost almost any concentrations.

ACKNOWLEDGMENTS

This work was supported by the National Science Foundation under Grant No. DMR-9321924. One of the authors (D.H.) was supported by the National Science Foundation Advanced Liquid Crystal and Optic Materials Under Grant No. DMR-8920147.

[1] J. S. Collura (private communication).
[2] D. J. Pine, D. A. Weitz, P. M. Chailin, and E. Herbolzheimer, Phys. Rev. Lett. **60**, 1134 (1988).
[3] S. Fraden and G. Maret, Phys. Rev. Lett. **65**, 512 (1990).
[4] D. J. Durian, D. A. Weitz, and D. J. Pine, Science **252**, 686 (1991).
[5] J. C. Earnshaw and A. H. Jaafar, Phys. Rev. E **49**, 5408 (1994).
[6] H. Stark and T. C. Lubensky, Phys. Rev. Lett. **77**, 2229 (1996).
[7] T. G. Mason and D. A. Weitz, Phys. Rev. Lett. **74**, 1250 (1995).
[8] M. H. Kao, K. Jester, A. G. Yodh, and P. J. Collings, Phys. Rev. Lett. **77**, 2233 (1996).
[9] D. G. Dalgleish and D. S. Horne, Milchwissenschaft **46**, 417 (1991).
[10] D. Weitz and D. Pine, in *Dynamic Light Scattering: The Method and Some Applications*, edited by W. Brown (Oxford, New York, 1993), pp. 652–720.
[11] P. Sheng, *Introduction to Wave Scattering, Localization, and Mesoscopic Phenomena* (Academic, New York, 1995).
[12] P. D. Kaplan, A. D. Dinsmore, A. G. Yodh, and D. J. Pine, Phys. Rev. E **50**, 4827 (1994).
[13] G. F. Bohren, Am. J. Phys. **55**, 524 (1987).
[14] S. Chandrasekhar, *Radiative Transfer* (Dover, New York, 1960).
[15] H. C. van de Hulst, *Multiple Light Scattering* (Academic, New York, 1980), Vol. 2.
[16] A. Ishimaru, *Wave Propagation and Scattering in Random Media* (IEEE/Oxford, New York, 1997), pp. 177–178.
[17] V. G. Kolinko, F. F. M. de Mul, J. Greve, and A. V. Priezzhev, Appl. Opt. **35**, 4541 (1996).
[18] A. E. Bailey and D. S. Cannell, Phys. Rev. E **50**, 4853 (1994).
[19] H. Stark and T. C. Lubensky, Phys. Rev. E **55**, 514 (1997).
[20] H. C. van de Hulst, *Multiple Light Scattering* (Ref. [15]), pp. 396–476.
[21] D. E. Koppel, J. Chem. Phys. **57**, 4814 (1972).
[22] C. F. Bohren and D. Huffman, *Absorption and Scattering of Light by Small Particles* (Wiley-Interscience, New York, 1983).
[23] M. Kerker, *The Scattering of Light and Other Electromagnetic Radiation* (Academic, New York, 1969).
[24] H. C. van de Hulst, *Multiple Light Scattering* (Ref. [15]), p. 313.
[25] *Photon Correlation and Light Beating Spectroscopy*, edited by H. Z. Cummins and E. R. Pike (Plenum, New York, 1974).
[26] B. J. Berne and R. Pecora, *Dynamic Light Scattering* (Wiley, New York, 1976).
[27] *Dynamic Light Scattering: Applications of Photon Correlation Spectroscopy*, edited by R. Pecora (Plenum, New York, 1985).
[28] *Dynamic Light Scattering: The Method and Some Applications*, edited by W. Brown (Oxford University Press, Oxford, 1993).
[29] *Light Scattering Principles and Development*, edited by W. Brown (Oxford University Press, Oxford, 1996).
[30] F. C. MacKintosh and S. John, Phys. Rev. B **40**, 2383 (1989).
[31] D. J. Durian, Appl. Opt. **34**, 7100 (1995).
[32] D. J. Durian, Phys. Rev. E **51**, 3350 (1995).
[33] M. J. Stephen and G. Cwilich, Phys. Rev. Lett. **59**, 285 (1987).
[34] M. J. Stephen, Phys. Rev. B **37**, 1 (1988).
[35] G. Maret and P. E. Wolf, Z. Phys. B **65**, 409 (1987).
[36] I. Edrei and M. Kaveh, J. Phys. C **21**, L971 (1988).
[37] Č. Koňák *et al.*, Appl. Opt. **30**, 4865 (1991).
[38] P. Štěpháne k, J. Chem. Phys. **99**, 6384 (1993).
[39] P. M. Saulnier and G. H. Watson, Opt. Lett. **17**, 946 (1992).
[40] H. R. Haller, C. Destor, and D. S. Cannell, Rev. Sci. Instrum. **54**, 973 (1983).
[41] M. F. Clapper, Master's thesis, John Carroll University, 1998 (unpublished).
[42] D. Harrison and M. R. Fisch, Langmuir **12**, 6691 (1996).
[43] P. R. Bevington and D. K. Robinson, *Data Reduction and Error Analysis for the Physical Sciences*, 2nd ed. (McGraw-Hill, New York, 1992).